Materials Today Communications 36 (2023) 106631

Contents lists available at ScienceDirect

Materials Today Communications

journal homepage: www.elsevier.com/locate/mtcomm

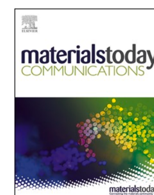

Solid-state reactions between iridium thin films and silicon carbide in the 700 °C to 1000 °C temperature range

E. Njoroge [a,b,*], T. Hlatshwayo [a], T. Mokgadi [a], T. Thabethe [a], V.A. Skuratov [c,d,e]

[a] Department of Physics, University of Pretoria, Pretoria, South Africa
[b] ENGAGE, University of Pretoria, Pretoria, South Africa
[c] Dubna State University, Dubna, Russia
[d] Joint Institute for Nuclear Research, Dubna, Russia
[e] National Research Nuclear University MEPhI, Moscow, Russia

ARTICLE INFO

Keywords:
Iridium
Silicides
Silicon carbide
RBS
GIXRD
Raman

ABSTRACT

The solid-state reactions between iridium thin films (50 nm) and 6H-SiC in the 700–1000 °C temperature range were investigated. The microstructure and surface morphology of the Ir thin films on 6H-SiC were examined using Rutherford backscattering spectrometry (RBS), scanning electron microscopy (SEM), Raman spectroscopy and grazing incidence X-ray diffraction (GIXRD). The electron beam deposited Ir films had a polycrystalline structure with the (111) preferred orientation and their crystallinity increased with annealing temperature. The Ir films were stable and did not interact with the SiC substrate after annealing at temperatures below 800 °C. The RBS results indicate that the initial reaction at 800 °C was very fast and almost the entire 50 nm film had reacted leading to the formation of Ir-rich silicides, Ir_3Si_2 and IrSi. After annealing at 900 and 1000 °C, the RBS profiles XRD results showed that the solid-state reactions proceeded further and Ir_3Si_2 was converted to IrSi. At the final annealing temperature of 1000 °C the predominant phase was IrSi. Thermodynamic analysis of the reaction phases confirmed the formation and sequence of the phases observed.

1. Introduction

Silicon carbide (SiC) is a ceramic material with a wide range of applications. This is due to its exceptional properties which are derived from the strong covalent bonds between the silicon and carbon atoms. These properties include high melting temperature, low neutron capture cross-section, wide band gap, excellent mechanical properties (high hardness, structural stability, high resistance to abrasion and erosion), high thermal conductivity, good thermal shock resistance, high corrosion resistance, high thermal stability, low coefficient of thermal expansion etc. [1,2]. These properties make SiC an important material in diverse areas of application as a; metal matrix composite material [1,3], wide bandgap semiconductor for microelectronic devices and sensors [4], high-temperature structural material for radiation harsh environments such as nuclear, aerospace applications and thermal protection systems [5].

In most of these high-temperature and radiation-harsh applications, some of the SiC properties can degrade when they are expected to remain exceptional. SiC is known to readily oxidize at high temperatures [2] and undergo structural damage in radiation-harsh environments [6]. The oxidation and radiation damage of SiC are critical issues which can limit the use of SiC-based materials. The successful and long-term use of SiC requires the control or prevention of oxidation and reduction of radiation damage. A direct solution to the problem is the introduction of a stable barrier or capping layer between SiC and the oxidizing or radiation-harsh environment [7].

The application of protective layers is one of the methods that can be applied to protect ceramic materials against oxidation or irradiation effects [8]. Refractory metals such as tungsten [7] and iridium [9,10] have been proposed as potential candidates for protective layers on SiC, ZrC and graphite. It is of critical importance that these metal-based protective layers should provide good mechanical, and thermochemical stability to the substrates. Additionally, they should also demonstrate good compatibility and adherence to the substrates. This requires the protective layers to be physically uniform and nonporous.

Iridium (Ir) is a refractory transition metal that belongs to the platinum group and is known to be the most corrosion-resistant metal [11]. Iridium has drawn considerable interest recently for high-temperature

* Corresponding author at: Department of Physics, University of Pretoria, Pretoria, South Africa.
E-mail address: eric.njoroge@up.ac.za (E. Njoroge).

https://doi.org/10.1016/j.mtcomm.2023.106631
Received 26 April 2023; Received in revised form 4 July 2023; Accepted 7 July 2023
Available online 9 July 2023
2352-4928/© 2023 The Authors. Published by Elsevier Ltd. This is an open access article under the CC BY-NC-ND license (http://creativecommons.org/licenses/by-nc-nd/4.0/).

structural material applications where it can act as a protective layer. It is a promising anti-oxidation protection material that can allow for higher service temperatures (up to 2000 °C), and longer service lifetime [12,13]. This interest in Ir is due to its intrinsic advantages, and a unique set of properties that make it a candidate for a wide range of highly demanding applications at elevated temperatures [3]. These properties include; a high melting temperature (2446 °C), high specific strength at high temperatures, remarkable oxidation resistance [3,12], low oxygen permeability and diffusivity at temperatures below 2370 °C (10^{-14} g•cm^{-1}·s^{-1} at 2200 °C) [1,3,13–15], high chemical stability, excellent mechanical strength [16], good electric and thermal conductivity [17,18], and corrosion resistance [19]. The properties of iridium make it the most promising candidate for use as a protective coating for structural materials, such as SiC, against extreme operating conditions including high temperatures, oxidizing and radiation harsh environments.

The iridium-SiC system, specifically as iridium thin films on silicon carbide, is of great interest for many applications. These include microelectronics, sensors [20], development of high-temperature materials having enhanced oxidation resistance [21], such as diffusion barriers for high temperature and radiation harsh environment applications. The effectiveness of Ir as a protective film and its structural integrity can be limited by several factors. This includes the coefficient of thermal expansion mismatch, especially at elevated temperatures. Although strong bonding between a protective film and the substrate can be obtained by solid-state reactions, extensive interface reactions and unfavourable reaction products may cause the degradation of the mechanical properties of the coating.

Compared to other platinum-group metals such as Pt, Ti, Zr, and Pd, the literature on research concerning reactions between iridium and silicon carbide is limited. Previous work on the solid-state reactions between Ir and SiC was performed using different types of starting materials, such as, Ir and SiC powders [20–23], Ir rod [24] and Ir films [25] on SiC substrates. These studies were performed at higher temperatures (1000–1900 °C) and the results showed the formation of a range of iridium silicides phases. The temperature of the initial reaction and initial silicide phases formed varied depending on the starting materials.

Iridium thin films deposited on silicon carbide are of great interest for the development of high-temperature materials with enhanced oxidation resistance. To assess the potential of Ir thin films as protective layers against oxidation and radiation damage of SiC substrates, it is essential to investigate the stability of the Ir-SiC interface and the reactions between Ir and SiC. The processes that occur in the Ir-SiC system at elevated temperatures are important and need to be well understood. A recent summary by [20] on Ir-SiC reactions at high temperatures indicates that previous research has focused on what can be considered as bulk interactions. The only study involving Ir films on SiC was conducted by [25] which examined films with a thickness range of 3.43–4.88 μm on CVD SiC. Therefore, to the best of our knowledge, no study has been conducted on Ir-SiC interactions at the thin film scale, that is < 1 μm. Solid-state reactions in the thin film case differ significantly from those involving bulk materials. The initial temperature of reaction, initial reaction phases formed and phase sequence usually differ from those involving bulk materials [26].

In this study, the solid-state reactions between thin (50 nm) Ir films and 6H-SiC substrates were investigated using a combination of grazing incidence X-ray diffraction (GIXRD), SEM, RBS and Raman spectroscopy techniques. The Ir-SiC samples were annealed at lower temperatures of 700 °C to 1000 °C in vacuum compared with the previous studies which were performed at higher temperature ranges. The aim of this study is to investigate the stability of Ir thin films deposited on SiC, as well as their surface morphology, interdiffusion, and the reaction mechanisms. This will include an examination of the temperature of initial reactions, the initial silicide phases formed, and the sequence of phase formation that occurs between the Ir thin films and SiC after vacuum annealing.

2. Experimental methods

Semi-insulating 6H-SiC (0001) single crystal substrates, double-side polished to < 0.5 nm RMS roughness from Xiamen Powerway Advanced Material Co., were used in this study. The 6H-SiC substrates were cut into 5 mm × 5 mm pieces, and then chemically cleaned in an ultrasonic bath to remove any contamination and the native oxide layer before loading them into the electron beam evaporation chamber. Iridium films were deposited on the SiC substrates by electron beam evaporation from a 99.9% pure Ir target. The e-beam chamber was evacuated to a base pressure of about 5×10^{-7} mbar before deposition and the pressure was about 8×10^{-6} mbar during the evaporation process. Prior to deposition, the Ir target was evaporated for about 10 min while the SiC substrates were shielded by the shutter. This step served to clean the Ir target by removing any surface contamination, stabilize the evaporation rate and for gettering. The Ir evaporation rate was about 0.2 Å/s and the thickness of the films was monitored in-situ by an Infincon meter until the required thickness of 50 nm was attained. Due to the difficulties with depositing iridium films, the 50 nm Ir film was prepared by performing sequential deposition (30 nm followed by 20 nm) without breaking the vacuum to avoid heating. This allowed the deposition to be done at room temperature and to avoid any interdiffusion or reactions occurring between the Ir thin films and the SiC substrate during deposition. The room temperature deposition also avoids any desorption effects on the deposited Ir film. The desorption rate of the incident Ir atoms has been reported to increase with substrate temperatures leading to thinner films [25].

After deposition, the Ir-SiC samples were subsequently annealed in a vacuum (10^{-6} mbar) using a water-cooled horizontally mounted quartz tube furnace from 700 °C to 1000 °C in steps of 100 °C for 30 min. The as-deposited and annealed Ir-SiC samples were analysed using Rutherford backscattering spectrometry (RBS) to determine the thickness of Ir film, the thickness of the reaction zone and the composition of the iridium silicide layers. The RBS measurements were performed using a 2 MeV $4He^{+}$ beam with a detector resolution of 15 keV, at a backscattering angle of 150°. The experimental RBS spectra were analyzed by simulating using the RUMP code [13]. The surface morphology of Ir-SiC samples was analyzed before and after vacuum annealing using a high-resolution field emission gun scanning electron microscope (FEG-SEM, Carl-Zeiss ULTRA-55) operating at accelerating voltage of 2 kV. The crystal structure, phase identification and orientation of the as-deposited and annealed Ir-SiC samples were determined by grazing incidence X-ray diffraction (GIXRD) using a Bruker D8 Advanced XRD system. The analysis was performed using a Cu (Kα) radiation source (λ = 0.1540598 nm) at a two-theta step size of 0.04°. The XRD patterns were measured at a grazing incidence angle of 3°. The XRD patterns were collected in the angular range of $25° < 2\theta < 90°$. The qualitative and quantitative phase analysis was performed using the International Centre for Diffraction Data (ICDD-PDF-2) database. Raman spectroscopy analysis was performed to verify the presence and form of carbon in the Ir-SiC samples before and after annealing using the HORIBA Jobin Yvon's T64000 series II triple spectrometer system. The Raman spectra were collected at room temperature using argon ion laser excitation (514.5 nm) through an Olympus microscope (objective ×50) at laser power of 10 mW.

3. Results

3.1. Rutherford backscattering spectrometry (RBS)

The experimental RBS spectrum for the as-deposited Ir-SiC sample and the corresponding RUMP simulation spectrum are displayed in Fig. 1(a). The arrows in Fig. 1(a) indicate the surface channel positions of Ir, Si and C at channel numbers 332, 217 and 104 respectively. The simulated Ir peak fitted well with the measured Ir profile indicating the successful deposition of Ir at room temperature. The layer consisted of

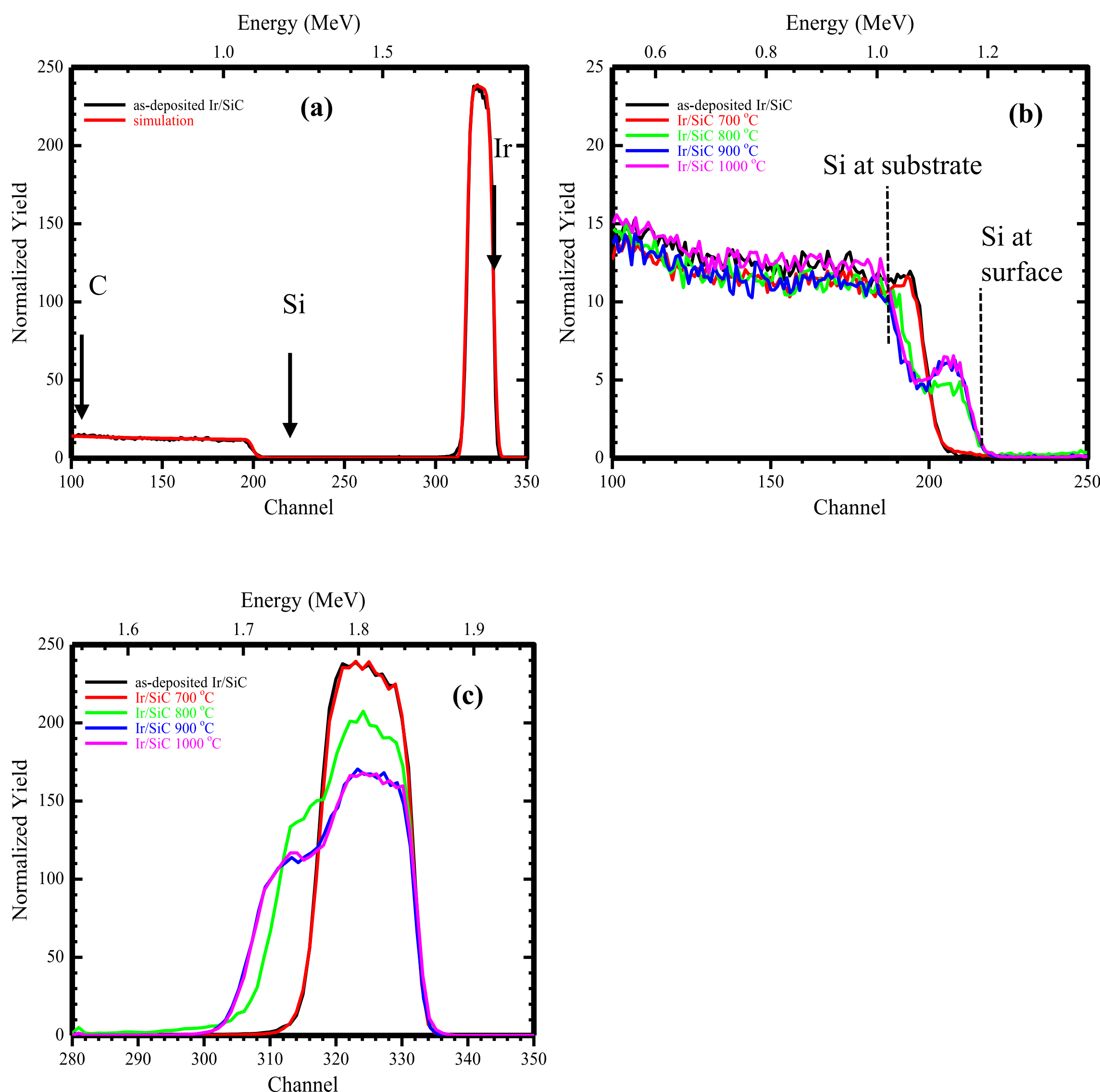

Fig. 1. (a) RBS spectra of as-deposited Ir-SiC sample and the corresponding RUMP simulation, RBS spectra of the as-deposited and samples annealed in vacuum at 700 °C, 800 °C, 900 °C and 1000 °C for 30 min (b) silicon signal and (c) Ir signal.

only iridium and had a thickness of about 358 × 10^{15} cm^{-2} which is about 50 nm (using the density of Ir = 22.51 g/cm^3 or 7.0527 ×10^{15} cm^{-2}). The thickness values of the as-deposited Ir film deduced from RUMP simulation and the in-situ method are in good agreement. The low signal between channel numbers 200–310 is indicates the absence of impurities in the deposited Ir film. The edge of the Si signal and Ir back edge are flat indicating that no intermixing between the Ir film and the SiC substrate occurred during deposition.

The RBS spectra of the as-deposited and annealed Ir-SiC samples are depicted in Fig. 1(b) and (c). The spectrum of the sample annealed at 700 °C is similar to that of the as-deposited sample, indicating that there was no interdiffusion or solid-state reactions at the Ir-SiC interface after annealing at this temperature. Therefore, the Ir thin film on the SiC substrate remained stable at 700 °C, and its thickness did not change. This is consistent with the reported negligible evaporation of iridium in vacuum at temperatures below 2100 °C [10].

Annealing the Ir-SiC samples at 800 °C resulted in a decrease in the Ir peak height and a shift of the back edge to lower energy channels, as seen in Fig. 1(c). Consequently, the Si edge shifted towards higher energy channels with a step appearing. The high energy edge of the Si signal now corresponds to the surface channel position for Si, as shown in Fig. 1(a) and (b). This indicates that interdiffusion or reactions at the Ir-SiC interface began at 800 °C accompanied by very fast interdiffusion rates at the interface. The composition profiles given in Fig. 2(b) show that the 50 nm Ir film had been consumed after annealing at 800 °C to form Ir silicides and carbon precipitates. A 965 × 10^{15} cm^{-2} wide reaction layer was observed on top of the SiC substrate. The composition profiles shown in Fig. 2(b) for the reaction zone after annealing at 800 °C also indicate that the Ir content is high in the layers near the surface but rapidly decreases from an Ir to Si ratio of 63.4:36.6 ($IrSi_x$ = 1.73) to about 10.2:38.5 in the layers next to the SiC substrate. The variation in the Ir, Si and C compositions indicates the presence of five major composition regions with silicide phases formed from the substrate to the sample surface, as the Si signal edge was observed at its surface channel position. The identification of the iridium silicides formed is discussed in the GIXRD results section.

Ir reacts with SiC through a decomposition process of the SiC substrate. The dissociated Si atoms diffuse towards the Ir layer and react to form one or more Ir-silicide(s) layer. The free carbon was mostly found between the SiC substrate and the Ir-silicide layer due to the low solubility of carbon in Ir [10]. This feature can be seen in Fig. 2(b) where the carbon concentration is highest near the SiC substrate and gradually

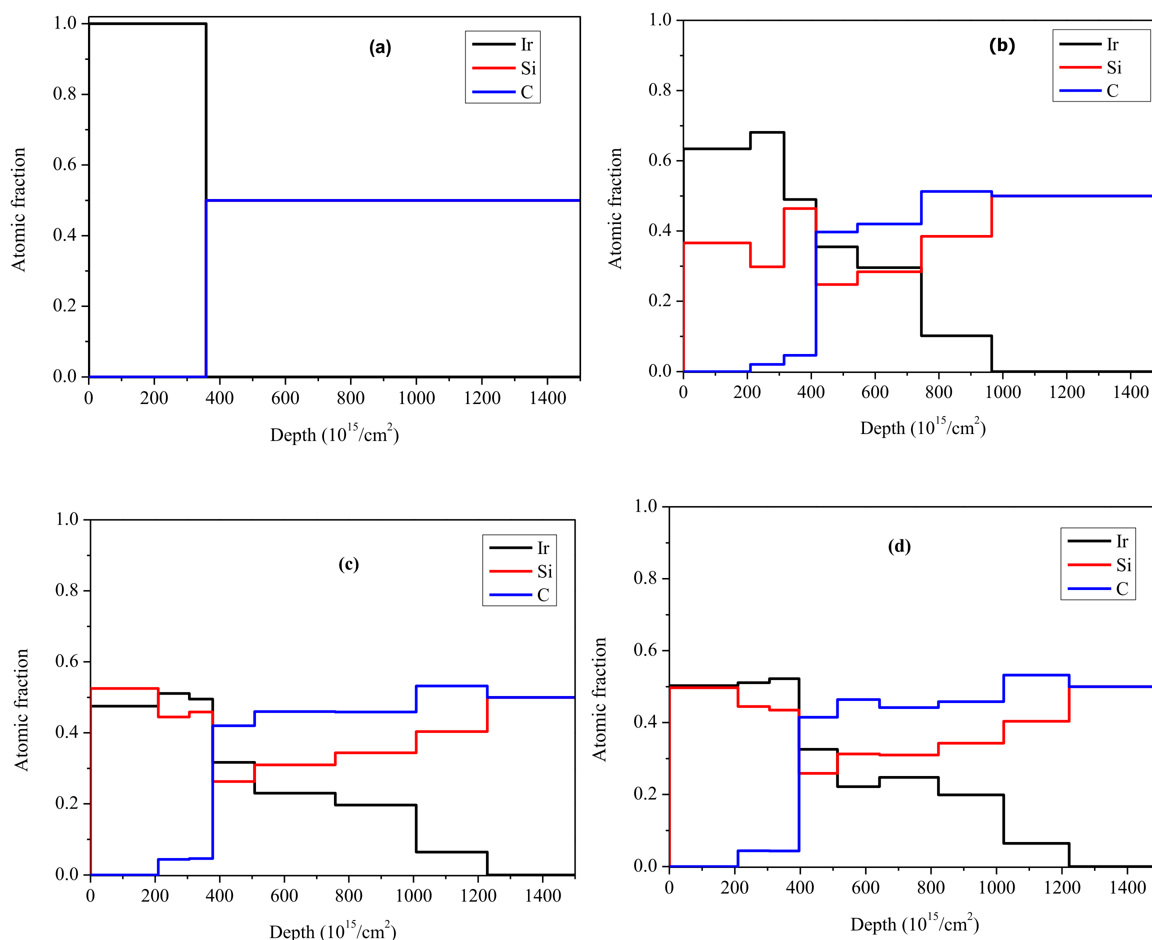

Fig. 2. Composition profiles obtained from RUMP simulations of the RBS spectra of (a) the as-deposited Ir-SiC sample and after annealing at (b) 800 °C (c) 900 °C and (d) 1000 °C for 30 min.

decreases towards the surface. The diffusion and solid-state reactions observed at 800 °C are in contrast to previous findings by other researchers who reported that reactions between Ir and SiC begin at 1000 °C [21,22]. However, it should be noted that they used different starting materials (Ir and SiC powders) which can be considered as bulk materials.

Increasing the annealing temperature to 900 °C caused a further decrease in the Ir peak height accompanied by further widening of the Ir peak towards lower energy channels as seen in Fig. 1(b). The Si step and the top of Ir peak are not flat, which indicates varying compositions of Ir, Si and C in the reaction zone. As shown in Fig. 1(a), the Si profile between channel numbers 200–220 has a higher yield compared to the sample annealed at 800 °C, indicating further diffusion of Si towards the surface leading to a higher concentration of Si atoms near the surface of the Ir-SiC sample. At about channel number 195, the Si profile has a lower yield, compared to the 800 °C profile. This could be due to the free carbon that originates from the decomposition of SiC and segregates near the SiC substrate. The amount of free carbon from the SiC substrate had increased in this region from 0.513 to 0.532 as seen in the composition profiles in Fig. 2(b) and (c). The total reaction zone thickness had increased to 1228×10^{15} cm^{-2}, and given that the initial Ir film was approximately 50 nm (358×10^{15} cm^{-2}) thick as determined by RBS analysis, it is clear that the reaction zone extends into the SiC substrate, see Fig. 2(c). The RBS spectra of the Ir-SiC samples annealed at 1000 °C for 30 min were similar to those annealed at 900 °C as seen in Fig. 1 and Fig. 2. Therefore, the reactions between the Ir thin film and SiC proceeded in the same manner and rate as in the sample annealed at 900 °C. A comparison of the composition profiles of the samples annealed at 800 °C, 900 °C and 1000 °C shows that near the sample's surface, the compositions seem to be converging toward an Ir to Si ratio of 50:50 with increasing annealing temperatures. The convergence of the composition profiles towards an Ir to Si ratio of 50:50, as observed in the samples annealed at 900 °C, and 1000 °C, suggests that the final reaction between Ir and SiC is likely to be Ir + SiC → IrSi + C.

It is difficult to draw any conclusions about the structural composition of the reaction zone from the RBS results. However, the composition profiles suggest that it could consist of IrSi with carbon precipitates, or IrSi + Ir silicides and carbon precipitates. Further analysis by GIXRD was performed to identify the phases formed and the phase evolution involved.

3.2. GIXRD analysis

Qualitative and quantitative phase analysis was performed by GIXRD analysis which allowed the determination of the crystallinity or structure of the Ir thin films deposited on 6H-SiC and identification of the reaction products in the Ir-SiC samples after annealing. The GIXRD patterns of the as-deposited and annealed Ir-SiC samples (700–1000 °C in vacuum for 30 min) are shown in Fig. 3. The grazing incidence angle was initially varied until the SiC peak intensity was low enough to ensure the Ir thin film and the reaction zone was sufficiently analysed.

The XRD patterns of the as-deposited Ir films were found to exhibit a polycrystalline structure, with broad Ir reflections at 40.82°, 47.41°, 69.54° and 83.65° 2θ positions corresponding to the (111), (200), (220) and (311) planes respectively, of the face centred cubic (FCC) Ir structure. The sharp, dominating reflection observed at 35.58° was indexed

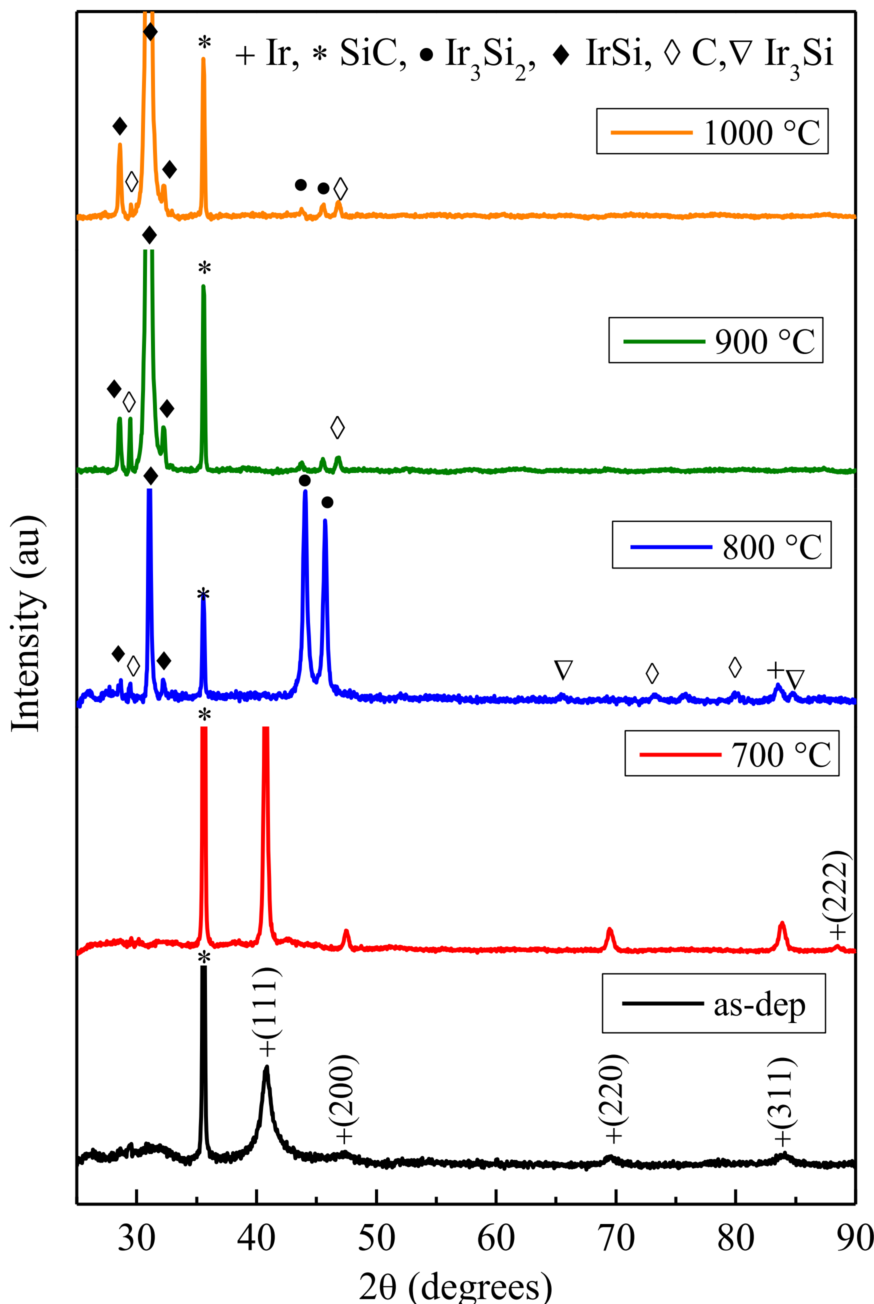

Fig. 3. GIXRD patterns of Ir thin films deposited on 6H-SiC then annealed at 700 °C, 800 °C, 900 °C and 1000 °C.

as the (0006) plane of the hexagonal polytype of the SiC substrate. This correlates with the observation from the RBS analysis that a pure Ir film was deposited on hexagonal SiC.

The preferential growth orientation was determined by calculating the texture coefficient ($TC_{(hkl)}$) using the Harris texture equation [9]:

$$TC_{(hkl)} = \frac{I_{(hkl)}/I_{o(hkl)}}{\frac{1}{N}\left[\sum_{i=1}^{N} I_{(hkl)}/I_{o(hkl)}\right]} \quad (1)$$

where $I_{(hkl)}$ is the measured intensity for the (hkl) plane, $I_{o(hkl)}$ is the standard peak intensity for the (hkl) plane and N is the number of diffraction peaks corresponding to diffracting (hkl) planes for Ir. Using Eq. (1) and the standard X-ray diffraction pattern of Ir, we determined that the TC(111), TC(200), TC(220) and TC(311) for the Ir thin film were 2.482, 0.592, 0.499 and 0.427, respectively. This indicates that the Ir films deposited on 6H-SiC by e-beam showed the presence of the preferred orientation of the Ir film along the (111) plane.

The preferred growth direction is governed by the minimization of the surface energy. Usually, the direction with the lowest surface energy grows faster. The surface free energies of Ir in the (100), (110) and (111) planes reported in [27] are 2.95 J/m^2, 3.19 J/m^2 and 2.59 J/m^2 respectively. Since Ir has an FCC structure, the (111) planes are close-packed in this unit cell and have the lowest surface energy. This explains why the (111) orientation is most favoured in the deposited polycrystalline Ir films, although other crystallographic orientations such as (100) and (110) are also present, albeit in smaller quantities. This observation is similar to the findings of other researchers who deposited Ir films using RF [16,25], DC [28] sputtering, ALD [14], CVD [29] on various substrates such as β-SiC, Si, SiO_2/Si. These results suggest that the preferred orientation during the growth of polycrystalline Ir films is hardly influenced by the underlying substrate.

The GIXRD patterns of the Ir-SiC samples annealed at 700 °C

exhibited similar reflections to the as-deposited sample and remained at the same 2θ positions, indicating no peak shift. Comparing the GIXRD patterns of the as-deposited sample with those of the sample annealed at 700 °C, significant increase in the intensity of the (111), (200), (220), (311) reflections can be observed, with the (111) peak remaining dominant. This suggests that the (111) reflection remained the preferential orientation of the Ir films at 700 °C. A low-intensity peak appeared at 88.65° which was indexed to the Ir (222) plane. The strong reflections observed in the polycrystalline Ir film are evidence of an increase in crystallinity after annealing at 700 °C. This increase is due to the higher atomic mobility which enables the thermodynamically favoured grains to grow [30]. The XRD patterns confirm the RBS results, indicating that no reactions occurred in the 700 °C annealed sample.

There were drastic changes in the XRD patterns after annealing the Ir-SiC samples at 800 °C. The Ir peaks observed at 40.82°, 47.41°, 69.54° and 88.65° 2θ positions after the 700 °C annealing disappeared after annealing at 800 °C, while the peak at 83.65° had a lower intensity indicating that a small fraction of pure Ir remained in the sample. The SiC peak at 35.58° was still present indicating that the reaction phases formed were evaluated from the sample surface to the SiC substrate. The RBS results show that the Ir-silicide/SiC interface moved towards the bulk implying that the thickness of the reaction zone was greater than that of Ir film. Several Ir silicide phases were found to be present in the sample, with the dominant peaks at 31.07° assigned to IrSi (011), at 44.05° and 45.73° assigned to Ir_3Si_2 (102) and Ir_3Si_2 (110), respectively. The low-intensity diffraction peaks at 28.67° and 32.22° were indexed to IrSi, while those at 65.46° and 84.72° were assigned to Ir_3Si. Fig. 3 also showed other weak diffraction peaks at 29.43°, 73.21°, and 79.93°. These peaks indicated the presence of carbon in the reaction zone of the sample annealed at 800 °C.

From the XRD results, it can be deduced that the reactive phase formation starts with the decomposition of SiC at 800 °C in the presence of Ir which yields Si and carbon. The Si reacts with Ir to form silicides while the carbon forms precipitates. As a result, a reaction zone forms on top of the SiC substrate consisting of mixed silicide phases, with Ir_3Si_2 and IrSi as the predominant silicide phases. The intensities of the Ir_3Si_2 and IrSi phases are higher than that of carbon therefore it can be assumed that the content of free carbon detected is less than that of Ir_3Si_2 or IrSi.

Increasing the annealing temperature to 900 °C and 1000 °C led to a drastic reduction in the intensity of the Ir_3Si_2 diffraction peaks at 44.05° and 45.73° 2θ positions and an increase in the intensity of the IrSi peak at 31.07°. This indicates that Ir_3Si_2 had been converted to IrSi during the second reaction stage that occurred at higher temperatures of 900 °C and 1000 °C. No reflections from Ir were observed indicating that all the Ir thin film had reacted to form silicides. The only difference after annealing at 1000 °C compared to 900 °C was the reduction in the intensity of the peaks at 29.47° and 32.25° which correspond to C and IrSi respectively. Analysis of the GIXRD patterns indicates that the structure of the silicide is consistent with orthorhombic IrSi with a preferred orientation in the (011) plane. The formation of IrSi as the final phase after annealing at 1000 °C in this study is similar to that of Yunfeng et al. [22] and Richards [25] at 1400 °C. The similarity in the diffraction patterns after annealing at 900 °C and 1000 °C suggests that the samples were in thermodynamic equilibrium. This is consistent with the Ir-Si-C phase diagram at 1340 °C [31], which shows that IrSi and SiC are in equilibrium and no further reactions are expected between them at these temperatures.

No IrO_2 reflections were detected in the sample annealed at 1000 °C since Ir is an oxidation-resistant metal. The composition profiles of the 900 and 1000 °C annealed samples in Fig. 2 had an Ir to Si ratio of 50:50 near the surface which suggests the formation of the IrSi phase. This observation correlates with the GIXRD results. The presence of the carbon peaks observed in the GIXRD analysis was confirmed by Raman analysis discussed in Section 3.4.

In this study, the solid-state reactions started at a lower temperature of 800 °C. This contradicts the observations of other researchers who reported that the initial reactions occur at higher temperatures ranging from 1000 °C to 1200 °C, depending on the different starting materials (e.g. powders at 1000 °C [22,22] and Ir bulk films on SiC at 1200 °C [25]). The initial phase observed in previous studies was primarily Ir_3Si at 1000–1100 °C [20–23], except for Richards [25] who found mostly IrSi with a trace of Ir_3Si at 1200 °C. The final phase(s) varied in the different studies, with some reporting Ir_3Si at 1200 °C [22], a mixture of Ir_3Si_2 + Ir_2Si + IrSi at 1300 °C [21], Ir_3Si at 1300 °C [20], and IrSi at 1400 °C [23] [25]. While in this study, the initial phases were Ir_3Si_2 and IrSi at 800 °C and the final phase observed was IrSi at 1000 °C. The differences in phases formed and temperature of the initial reaction observed in this study compared to the previous studies are due to the influence of the initial Ir and SiC structures which include particle size, high surface area and crystal lattice perfection or imperfection [21]. These factors may lead to the formation of some intermediate phases in the thin films case, as reported in other studies [32].

Reactive phase formation in thin films is known to differ from bulk diffusion couples. Interdiffusion and reaction processes in thin films generally occur over short annealing durations and at lower temperatures compared to bulk. This is due to the presence of high densities of short circuits for diffusion such as grain boundaries and dislocations [26]. The non-equilibrium phenomenon is governed by the competition between kinetic and thermodynamic factors. This explains the formation of Ir_3Si_2 at 800 °C as an intermediate phase, although IrSi is the thermodynamically favoured phase to form. The results from previous studies showed that the Ir silicide phases that form have Si content less than 50 at%, namely Ir_3Si, Ir_2Si, Ir_3Si_2 and IrSi. These reaction phases are similar to those observed in this study after annealing over the entire temperature range of 800–1000 °C.

3.3. SEM analysis

For applications involving protective films, it is important to consider the morphology of the Ir thin film, as it strongly influences its protective abilities. Fig. 4(a) shows the SEM micrographs of the surface morphology of the 50 nm Ir thin films deposited in 6H-SiC before and after annealing. The as-deposited thin films are dense, very smooth and homogeneous, without any surface defects such as pores or cracks and no grain boundaries visible. This indicates a uniform deposition, which is typical of low-temperature deposition. Fig. 4(b) to (e) display the plan-view SEM images of the surface morphology of the Ir-SiC samples annealed at temperatures ranging from 700–1000 °C.

The surface morphology of the Ir film did not change significantly after annealing at 700 °C compared to the as-deposited film surface. The RBS analysis across the Ir/SiC interface of the sample annealed at 700 °C, showed no evidence of interdiffusion across the Ir film and SiC substrate. The surface of the Ir film remained smooth and featureless. In contrast, the morphology of the sample annealed at 800 °C exhibits a surface consisting of closely packed, homogeneous and spherically shaped grains (granular surface). Formation of the granular structures at 800 °C indicates that solid-state reactions between Ir thin film and SiC had occurred leading to the formation of a reaction zone extending from the SiC substrate to the sample surface eliminating any trace of the as-deposited morphology. Since the granular structures appear after the reactions at 800 °C, the granular surface consists of the Ir silicide phases identified by GIXRD analysis. The granular surface morphology after annealing is due to atomic migration, phase nucleation and grain growth.

At higher annealing temperatures of 900 °C and 1000 °C, the SEM micrographs show almost identical granular surface morphologies to those annealed at 800 °C. The SEM images in Fig. 4(c) to (e) show surface morphologies that are free of cracks or delamination even after annealing at the highest temperature of 1000 °C. The Ir silicide layers identified by GIXRD remained bonded to the SiC substrate.

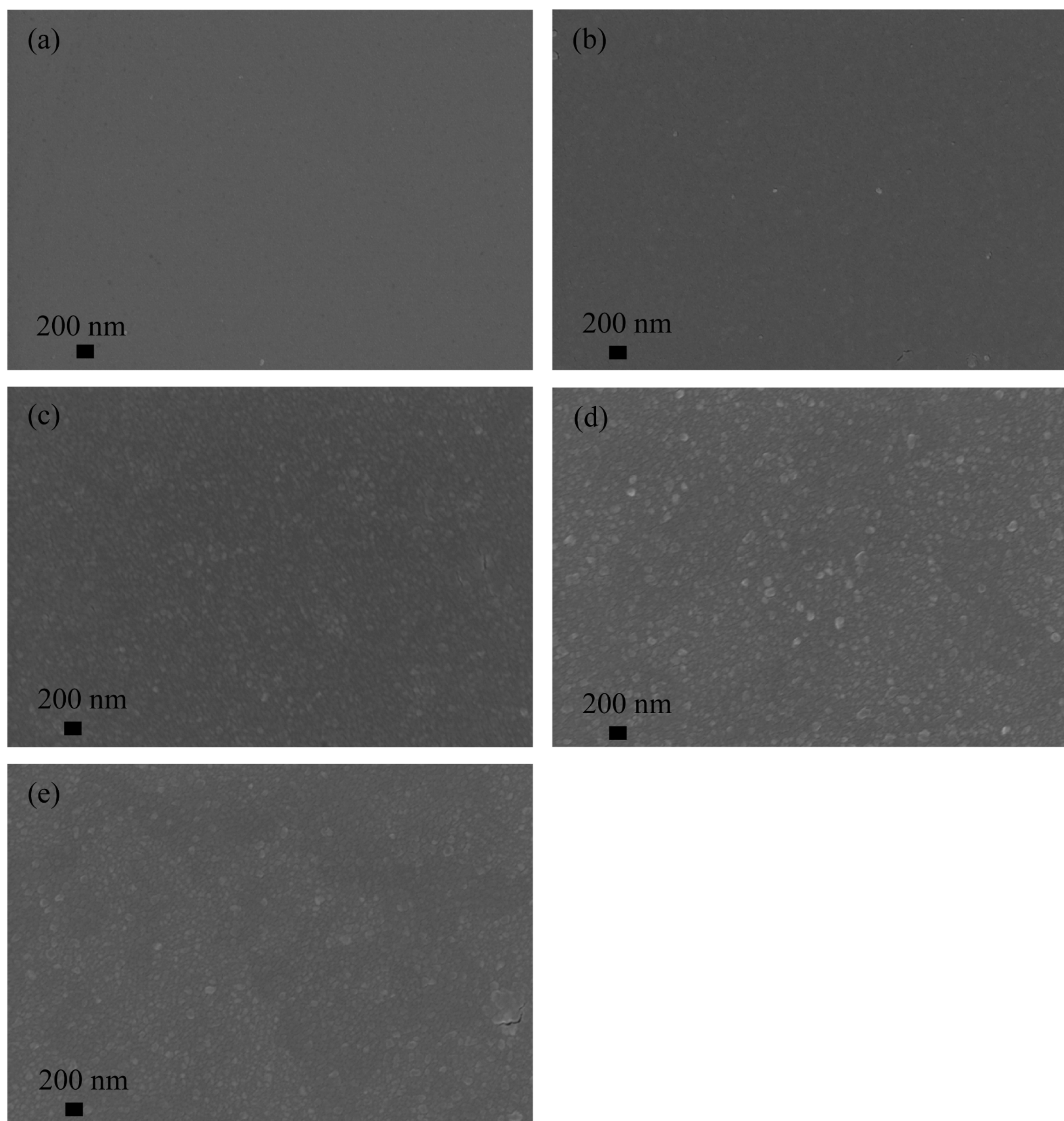

Fig. 4. SEM micrographs of the Ir films deposited on 6H-SiC, (a) as-deposited, after annealing at (b) 700 °C, (c) 800 °C, (d) 900 °C and (e) 1000 °C in vacuum.

3.4. Raman Spectroscopy

Raman spectroscopy is a contactless and non-destructive analysis technique that is known to be sensitive in characterizing the different allotropes of carbon. It was used to characterize the structure of carbon formed during the solid-state reactions between the Ir thin film and SiC substrate after annealing at 700–1000 °C. The Raman spectra of the as-deposited and annealed Ir-SiC samples, measured from the top surface, are shown in Fig. 5 in the 1000–2000 cm^{-1} spectral range.

The Raman spectrum of the as-deposited Ir layer shows no Raman peaks which is typical for Ir films. The Ir layer thickness prevented the laser beam from reaching the substrate, therefore, the 6H-SiC Raman bands were not observed. The spectrum of the Ir-SiC sample annealed at 700 °C (not shown here) does not exhibit any carbon Raman bands and is similar to the as-deposited one. This observation correlates with the GIXRD results which showed that solid-state reactions between Ir and SiC had not occurred at 700 °C. Another factor could be that the laser could not penetrate to the Ir-SiC interface to detect any carbon formed from the dissociation of SiC at 700 °C. However, the latter can be ruled out since RBS and XRD analysis did not show any evidence of reactions within the detection limits.

In contrast, all the Raman spectra obtained from the samples annealed at 800 °C, 900 °C and 1000 °C were similar and had two broad bands centered at 1347 cm^{-1} and 1597 cm^{-1} known as the first-order *D* and *G* bands, respectively. The *D* band is generally thought to be an indication of long-range disorder or defective hexagonal planar graphitic structures while the *G* band originates from the stretching vibrations in the basal plane of ideal graphite. The two broad (*D*) and (*G*) bands are similar to those of moderately damaged glassy carbon [33] and they are generally regarded as an indication of nanosized disordered graphitic clusters.

One of the reaction products from the solid-state reactions between Ir and SiC after annealing from 800 °C to 1000 °C is carbon. This is evident from the low-intensity carbon peaks observed in the GIXRD analysis and corroborated by Raman analysis. As stated in previous sections (RBS and GIXRD), the reactions were very fast, with the reaction zone extending from the SiC substrate to the sample surface. The decomposition reaction between Ir and SiC started at the interface at 800 °C and the volume

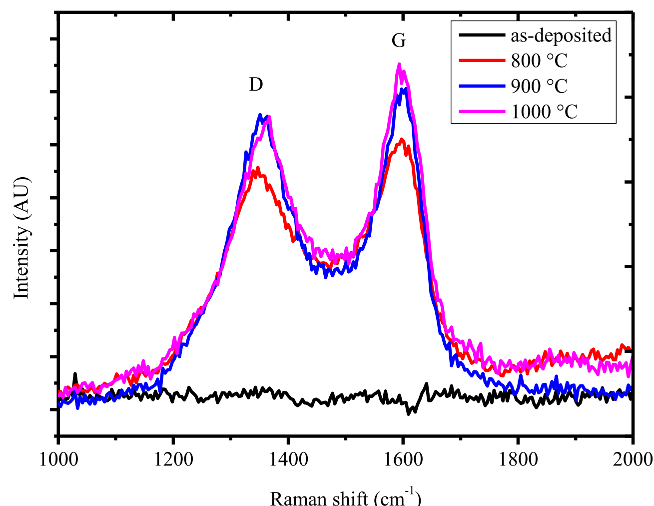

Fig. 5. Raman spectroscopy spectra in the 1000 – 2000 cm^{-1} spectral ranges of Ir-SiC samples before and after annealing at 800 °C, 900 °C and 1000 °C.

of the carbon clusters formed was sufficient enough to be detected by Raman spectroscopy. Carbon precipitated in course of the reactions and formed a solution with Ir silicides, therefore the degree of graphitization was limited.

The analysis of the Raman spectroscopy results was carried out by fitting the acquired spectra with a Lorentzian function for the *D* peak and a Breit-Wigner-Fano function (BWF) for the *G* peak. The fitting enabled the extraction of parameters such as the *D* and *G* peak positions, and their intensities. The I_D/I_G intensity ratios were calculated and compared. It is well known that the I_D/I_G intensity ratio can be used to estimate the size of graphitic crystallites or to deduce the degree of disorder in graphitic materials. The deconvolution of the *D* and *G* peaks revealed that the *D* peak position shifted to higher wavenumbers from 1347 cm^{-1} to 1367 cm^{-1} after annealing from 800 °C to 1000 °C but no shift in the G peak position was observed (see Fig. 5). The slight shift in the *D* band towards higher frequency implies a slight increase in the size of the nanocrystalline graphitic domains [34].

The I_D/I_G ratio was observed to slightly decline (from 0.9695 to 0.8555) with the increase in annealing temperature. A lower I_D/I_G ratio is indicative of a larger crystallite size or a higher degree of graphitization. The average in-plane crystallite size L_a was estimated by the Tuinstra–Koenig equation; $I_D/I_G = C_\lambda/L_a$, where $C_\lambda = 44$ Å for the excitation wavelength of $\lambda = 514.5$ nm. The graphitic crystallite size was deduced to increase from 4.5 nm to 5.1 nm after annealing from 800 °C to 1000 °C, respectively. This reveals the nanocrystalline structure of the graphitic clusters and a slightly larger size of the graphitic clusters with the increase in temperature. This suggests that an increase in the annealing temperature results in the formation of larger graphitic clusters and less disordered carbon structures.

4. Discussion

It is of interest to investigate if the reaction phases formed in this study correlate with thermodynamic considerations. Based on the previous research and the Ir-Si-C ternary phase diagram [31] it can be concluded that Ir and SiC are not in thermodynamic equilibrium. This is evident from the absence of a tie line between Ir and SiC in the phase diagram. Furthermore, no ternary phases between iridium, silicon and carbon (carbo-silicides) nor Ir carbides have been previously reported to form in reactions involving Ir and SiC. Therefore, the ternary phase diagram can be considered relatively simple. However, based on the Ir-Si phase diagram [35], several Ir silicides can form as reaction products in the Ir-Si section of the ternary phase diagram. These include Ir_3Si, Ir_2Si, Ir_3Si_2, IrSi, Ir_3Si_4, $IrSi_2$ and $IrSi_3$.

The thermodynamic data for iridium silicides is limited, with some values missing from the literature altogether. The enthalpies of formation at 25 °C can serve as a good approximation up to 1000 °C since they are not expected to vary significantly. Utilizing the enthalpy of formation data for iridium silicides compiled by Pretorius et al. [36], Searcy [31], and Golosov et al. [20], we were able to calculate the enthalpies of reactions associated with the formation of the Ir silicides. To ensure the reliability of our analysis, the data from each single source were used individually since the values reported vary significantly among different sources. From the enthalpies of formation data reported, it was observed that IrSi has the most negative formation enthalpy value but it is not the first phase observed to form in the previous and in this study as indicated in Section 3.2. The possible chemical reactions between Ir and SiC to produce Ir silicides and carbon can be expressed as shown in Table 1.

The reactions in Table 1 can be used to determine whether a reaction is thermodynamically possible or not. A negative value of the reaction enthalpies is required for the reaction to proceed. Based on the thermodynamic calculations, it was found that the reactions to form Ir-rich silicides, which have Si content < 50 at% (Ir_3Si, Ir_2Si, Ir_3Si_2, IrSi), are favourable, as their enthalpies of reaction are negative. Conversely, the enthalpies of reaction for Si-rich silicides, which have Si content > 50at % (Ir_3Si_4, $IrSi_2$, and $IrSi_3$), are positive, and these reactions are not expected to proceed spontaneously. The thermodynamic analysis results agree with the GIXRD results from this study and previous work, where only Ir-rich silicides form.

The initial reaction in this study occurred at a lower temperature of 800 °C, and the reaction products were identified by GIXRD analysis as a mix of Ir-rich silicides, predominantly Ir_3Si_2 along with IrSi. The final phase and most stable phase formed in this study was observed to be IrSi at 900 °C and 1000 °C after iridium had been completely consumed. This result is similar to those reported by Richards [25] and Yunfeng et al. [22], albeit at a higher temperature of 1400 °C after the Ir film and powder had fully reacted.

In previous work on reactions between Ir and SiC powders, Bannykh et al. [21] observed Ir_3Si_2 +Ir_2Si+IrSi at 1300 °C then IrSi appeared at 1400 °C, while Golosov et al. [23] observed Ir_3Si_2 + Ir_2Si at 1300 °C and IrSi+ Ir_3Si_2 at 1400 °C with IrSi as the predominant phase. In these previous studies, Ir had not completely reacted in the temperature range of 1200–1400 °C. We speculate that the enthalpies of formation may vary especially at temperatures exceeding 1000 °C or some phases such as Ir_3Si are favoured under certain kinetic conditions. This could explain why Ir_3Si was observed to form at temperatures of 1000–1200 °C while Ir is still available for reactions [20–23].

The difference between our results and those from previous studies may be attributed to several factors that influence the reactivity of Ir with SiC such as particle size and crystal lattice perfection. In the case of solid-state reactions involving thin film, the reaction pathway can differ significantly from those involving bulk materials [26]. The reactions often occur at lower temperatures and involve different initial phases or phase formation sequences. Typically, the initial phases formed in thin film solid-state reactions are not the most thermodynamically favoured. This is due to favourable kinetic factors such as diffusivities of Ir, Si, and C through the Ir silicides formed in the reaction zone.

Table 1
The reactions enthalpies for the iridium silicides calculated using ΔH°298 values obtained from a [31], b [36], and c [20].

Reaction	ΔH°$_R$ (kcal/g at)[a]	ΔH°$_R$ (kJ/mol at)[b]	ΔH°$_R$ (kJ/mol at)[c]
$3Ir + SiC \rightarrow Ir_3Si + C$	-3.4	-	-59.9
$2Ir + SiC \rightarrow Ir_2Si + C$	-3.0	-36.2	-51.9
$3Ir + 2SiC \rightarrow Ir_3Si_2 + 2C$	-7.5	-56.9	-65.6
$SiC + Ir \rightarrow IrSi + C$	-1.0	-9.5	-57.3
$3SiC + 2Ir \rightarrow Ir_2Si_3 + 3C$	8.0	47.1	-
$2SiC + Ir \rightarrow IrSi_2 + 2C$	11.7	67.8	-
$3SiC + Ir \rightarrow IrSi_3 + 3C$	26.6	168.2	99.64

Thin film solid state interaction is a non-equilibrium process and the effective concentration at the growth interface is independent of the relative thicknesses of the interacting components. The presence of carbon in the reaction zone from the dissociated SiC would shift the effective concentration towards the Ir-rich side where the Ir_3Si, Ir_2Si, Ir_3Si_2 and IrSi phases are favoured to form.

The XRD results of the Ir deposited on SiC and then annealed at 700 °C indicate that iridium oxide and SiO_2 were not formed in the Ir thin films. This is due to the Ir protective layer which is practically impermeable to oxygen at temperatures below 2000 °C [1,10]. At temperatures of 800–1000 °C after the Ir film had been consumed in the reactions to form Ir silicides, no Ir oxide nor SiO_2 formed. Iridium silicides have been reported to exhibit good high-temperature oxidation resistance comparable to that of $MoSi_2$ [1,37]. This ensured that the underlying SiC substrate did not get oxidised. Therefore, the iridium silicides layers formed on top of the SiC substrate can act as an additional diffusion barrier to oxygen [38].

A common limiting factor for protective films is the poor bonding between the coating and the substrate. Delamination can occur after deposition or at high temperatures if coefficients of thermal expansion (CTE) mismatch exist or if no chemical bonds exist at the interface of the film and the substrate [39]. Therefore a protective layer should have a coefficient of thermal expansion compatible with the substrates [10]. The average coefficients of thermal expansion for 6H-SiC along the a- and c-direction over the temperature range of 20–1000 °C are 4.46×10^{-6}/°C and 4.16×10^{-6}/°C, respectively [40]. While that of iridium from 30 °C to 865 °C is 7.33×10^{-6}/°C [41]. The values of the coefficients of thermal expansion for the Ir silicides observed in this study given in [20] are; $Ir_3Si = 8.7 \times 10^{-6}$ /°C, $Ir_3Si_2 = 7.6 \times 10^{-6}$/°C and $IrSi = 3.2 \times 10^{-6}$/°C. The slight mismatch between the Ir silicides and SiC CTE values would lead to some stress between the layers. However, no micro-cracks or delamination was observed in the Ir-SiC before and after annealing up to 1000 °C.

The application of iridium as a protective layer SiC is only limited by its high cost and scarcity. Therefore, it can only be used for critical applications such as in nuclear reactors or radiation harsh applications as a coating against oxidation at high temperatures, composite materials for heat-resistant components in nuclear power plants [21].

5. Conclusions

We investigated the solid-state reactions of thin iridium films deposited on hexagonal silicon carbide in the temperature range of 700–1000 °C in vacuum. This was done to gain insight into the viability of using Ir films as protective layers on SiC for use in radiation harsh, high temperatures or oxidizing environments. The as-deposited Ir thin films had a polycrystalline structure with the (111) preferred orientation. The Ir films were dense, had good adhesion to the SiC substrates and were without any visible defects. The Ir-SiC samples were observed to be stable with no evidence of reactions after annealing at temperatures of up to 700 °C in vacuum. Based on the GIXRD analysis the Ir films appear to have increased crystallinity after annealing at 700 °C. Based on this, we can deduce that Ir is a promising material which can provide stable anti-oxidation protection to SiC at temperatures below 700 °C.

The solid-state reactions between the Ir thin film and SiC were observed to start at 800 °C. A mixed reaction zone layer consisting of iridium-rich silicides (Ir_3Si_2, IrSi and Ir_3Si) and carbon. The solid-state reactions were very fast since Si was observed at the surface of Ir-SiC samples after annealing at 800 °C for 30 min. After the Ir film had completely reacted with SiC at 900 and 1000 °C, IrSi was the predominant phase formed. The solid-state reactions to form Ir silicides may consist of two stages. In the initial stage at 800 °C the reaction kinetics are controlled by the supply of Ir and the decomposition of SiC to supply Si to form Ir_3Si_2, IrSi and traces of Ir_3Si. During the second stage at 900 and 1000 °C when the supply of Ir was limited, IrSi was the main silicide phase formed.

The carbon is released from the SiC during the solid-state reactions at 800, 900 and 1000 °C was identified by Raman analysis to be in a graphitic state. The Ir silicides formed as reaction products are also adherent to the SiC substrate and they provide good oxidation resistance. Since the melting points of the iridium silicides are high (Ir_3Si, Ir_2Si and Ir_3Si_2 are close to 1400 °C), they can be used for high-temperature applications close to 1400 °C.

Declaration of Competing Interest

The authors declare the following financial interests/personal relationships which may be considered as potential competing interests: Eric Njoroge reports financial support was provided by National Research Foundation.

Data Availability

Data will be made available on request.

Acknowledgements

The authors are grateful to Dr T Ntsoane (Necsa) for the XRD measurements, Dr M Madhuku (iThemba LABS) for the RBS measurements and the National Research Foundation (NRF) of South Africa for funding (grant number 129601).

References

[1] A. Camarano, D. Giuranno, J. Narciso, SiC-IrSi3 for high oxidation resistance, Materials vol. 13 (2020) 1–11.
[2] J. Roy, S. Chandra, S. Das, S. Maitra, Oxidation behaviour of silicon carbide - a review, Rev. Adv. Mater. Sci. vol. 38 (2014) 29–39.
[3] A.D. Camarano, D. Giuranno, J. Narciso, New advanced SiC-based composite materials for use in highly oxidizing environments: synthesis of SiC/IrSi3, J. Eur. Ceram. Soc. vol. 40 (2020) 603–611.
[4] C. Bur, M. Bastuck, A. Schütze, J. Juuti, A.L. Spetz, M. Andersson, Characterization of ash particles with a microheater and gas-sensitive SiC field-effect transistors, J. Sens. Sens. Syst. vol. 3 (2014) 305–313.
[5] A.R. Powell, L.B. Rowland, SiC materials - progress, status, and potential roadblocks, Proc. IEEE vol. 90 (2002) 942–955.
[6] T.T. Hlatshwayo, et al., Effect of Xe ion (167 MeV) irradiation on polycrystalline SiC implanted with Kr and Xe at room temperature, J. Phys. D. Appl. Phys. vol. 48 (2015), 465306.
[7] T.T. Thabethe, T.T. Hlatshwayo, E.G. Njoroge, T.G. Nyawo, T.P. Ntsoane, J. B. Malherbe, Interfacial reactions and surface analysis of W thin film on 6H-SiC, Nucl. Instrum. Methods Phys. Res. Sect. B vol. 371 (2016) 235–239.
[8] M. Aparicio, A. Duran, Yttrium silicate coatings for oxidation protection of carbon – silicon carbide composites, J. Am. Ceram. Soc. vol. 83 (2000) 1351–1355.
[9] B.A.B. Alawad et al., Phase Formation between Iridium Thin Films and Zirconium Carbide Prepared by Spark Plasma Sintering at Relatively Low Temperatures, in Open Innovations Conference, 2018, pp. 265–270.
[10] J.M. Criscione, R.A. Mercuri, E.P. Schram, A.W. Smith, H.F. Volk, “High temperature protective coatings for graphite: Part II,” Ohio, 1964.
[11] S.B. Singh, Iridium chemistry and its catalytic applications: a brief review, Green. Chem. Technol. Lett. vol. 2 (2016) 206–210.
[12] L. Zhu, S. Bai, H. Zhang, Y. Ye, Y. Tong, Comparative investigation of iridium coating electrodeposited on molybdenum, rhenium and C/C composite substrates in molten salt in the air atmosphere, Phys. Procedia vol. 50 (2013) 238–247.
[13] K. Mumtaz, J. Echigoya, M. Taya, Preliminary study of iridium coating on carbon/carbon composites, J. Mater. Sci. vol. 28 (20) (1993) 5521–5527.
[14] T. Aaltonen, M. Leskela, Atomic layer deposition of iridium thin films, J. Electrochem. Soc. vol. 151 (2004) G489–G492.
[15] T. Chou, Solid state reactions between MoSi2 and Ir, Scr. Metall. Mater. vol. 24 (1990) 1131–1136.
[16] M.A. El Khakani, M. Chaker, B. Le Drogoff, Iridium thin films deposited by radio-frequency magnetron sputtering, J. Vac. Sci. Technol. A vol. 16 (1998) 885–888.
[17] M.R. Behfrooz, Study of Iridium (Ir) thin films deposited on to SiO2 substrates, J. Sci. Islam. Repub. Iran. vol. 16 (2005) 175–182.
[18] X. Yan, Q. Zhang, X. Fan, New MOCVD precursor for iridium thin films deposition, Mater. Lett. vol. 61 (2007) 216–218.
[19] E.K. Ohriner, Processing of iridium and iridium alloys, Platin. Met. Rev. vol. 52 (2008) 186–197.
[20] M.A. Golosov, V.V. Lozanov, A. Titov, N.I. Baklanova, Toward understanding the reaction between silicon carbide and iridium in a broad temperature range, J. Am. Ceram. Soc. vol. 104 (2021) 6653–6669.

[21] D.A. Bannykh, M.A. Golosov, V.V. Lozanov, N.I. Baklanova, Effect of mechanical activation of iridium on its reaction with refractory carbides, Inorg. Mater. vol. 57 (2021) 879–886.
[22] H. Yunfeng, L. Zhengxian, D. Jihong, H. Chunliang, Solid state reaction of Ir with SiC and Ir with Y2O3, Rare Met. Mater. Eng. vol. 41 (2012) 1149–1152.
[23] M. Golosov, V. Lozanov, N. Baklanova, The study of the iridium – silicon carbide reaction by Raman and IR spectroscopy, Mater. Today Proc. vol. 25 (2020) 352–355.
[24] A. Camarano, J. Narciso, D. Giuranno, Solid state reactions between SiC and Ir, J. Eur. Ceram. Soc. vol. 39 (2019) 3959–3970.
[25] M.R. Richards, Process Development for lrAl Coated SiC-C Functionally Graded Material for the Oxidation Protection of Graphite, University of Washington, 1996.
[26] J. Philibert, Reactive diffusion in thin films, Appl. Surf. Sci. vol. 53 (1991) 74–81.
[27] M.J. Mehl, D. Papaconstantopoulos, Applications of a tight-binding total energy method for transition and noble metals: elastic constants, vacancies, and surfaces of monatomic metals, Phys. Rev. B Condens. Matter Mater. Phys. vol. 54 (1996) 4519–4530.
[28] L. Trupina, et al., Growth of highly textured iridium thin films and their stability at high temperature in oxygen atmosphere, J. Mater. Sci. vol. 51 (2016) 8711–8717.
[29] J. Goswami, C.-G. Wang, P. Majhi, Y.-W. Shin, Highly (111)-oriented and conformal iridium films by liquid source metalorganic chemical vapor deposition, J. Mater. Res. vol. 16 (2001) 2192–2195.
[30] Y. Gong, C. Wang, Q. Shen, L. Zhang, Effect of annealing on thermal stability and morphology of pulsed laser deposited Ir thin films, Appl. Surf. Sci. vol. 254 (2008) 3921–3924.
[31] A.W. Searcy, L.N. Finnie, Stability of solid phases in the ternary systems of silicon and carbon with rhenium and the six platinum metals, J. Am. Ceram. Soc. vol. 35 (1962) 268–273.
[32] C.-H. Jan, C.-P. Chen, Y.A. Chang, Growth of intermediate phases in Co/Si diffusion couples: bulk versus thin-film studies, J. Appl. Phys. vol. 73 (1993) 1168–1180.
[33] E.G. Njoroge, et al., Effect of thermal annealing on SHI irradiated indium implanted glassy carbon, Nucl. Instrum. Methods Phys. Res. Sect. B vol. 502 (2021) 66–72.
[34] A.C. Ferrari, J. Robertson, Interpretation of Raman spectra of disordered and amorphous carbon, Phys. Rev. B vol. 61 (2000) 95–107.
[35] H. Okamoto, Ir-Si (Iridium-Silicon), J. Phase Equilibria Diffus. vol. 28 (2007) 495.
[36] P. Pretorius, T.K. Marais, C.C. Theron, Thin film compound phase formation sequence: an effective heat of formation model, Mater. Sci. Rep. vol. 10 (1993) 1–83.
[37] R. Novakovic, S. Delsante, D. Giuranno, Design of composites by infiltration process: a case study of liquid Ir-Si Alloy/SiC systems, Materials vol. 14 (2021) 18–23.
[38] S.T. Prisbrey and S.P. Vernon, Iridium/Iridium Silicide as an Oxidation Resistant Capping Layer for Soft X-ray Mirrors, Livermore, 2004.
[39] W. Wu, Z. Chen, Iridium coating: processes, properties and application. Part I, Johns. Matthey Technol. Rev. vol. 61 (2017) 16–28.
[40] Z. Li, R. Bradt, Thermal expansion of the hexagonal (6H) polytype of silicon carbide, J. Am. Ceram. Soc. vol. 69 (1986) 863–866.
[41] H.P. Singh, Determination of thermal expansion of germanium, rhodium, and iridium by X-rays, Acta Crystallogr. Sect. A vol. 24 (1967) 469–471.